

Infrared emission spectroscopy as a reliability tool

Q. Kim and S. Kayali
Jet Propulsion Laboratory
California Institute of Technology
4800 Oak Grove Drive, MS 303-210
Pasadena California 91109
Tel. (818) 354-6080
Fax (818) 393-0045
Email: Quiesup.Kim@jpl.nasa.gov

Abstract

In this paper, we report on a non-destructive technique, based on IR emission spectroscopy, for measuring the temperature of a hot spot in the gate channel of a GaAs metal/semiconductor field effect transistor (MESFET). A submicron-size He-Ne laser provides the local excitation of the gate channel and the emitted photons are collected by a spectrophotometer. Given the state of our experimental test system, we estimate a spectral resolution of approximately 0.1 Angstroms and a spatial resolution of approximately 0.9 μm , which is up to 100 times finer spatial resolution than can be obtained using the best available passive IR systems. The temperature resolution ($<0.02 \text{ K}/\mu\text{m}$ in our case) is dependent upon the spectrometer used and can be further improved. This novel technique can be used to estimate device lifetimes for critical applications and measure the channel temperature of devices under actual operating conditions. Another potential use is cost-effective prescreening for determining the 'hot spot' channel temperature of devices under normal operating conditions, which can further improve device design, yield enhancement, and reliable operation. Results are shown for both a powered and unpowered MESFET, demonstrating the strength of our infrared emission spectroscopy technique as a reliability tool.

Introduction

Thermal and mechanical failures on ICs in interconnect metallization and multilayer structures of advanced microelectronic devices have been recognized in the application of many commercial, military and space projects. Thermal degradation induces electrical and mechanical stress on power transistors. Precise knowledge of the local channel temperature of a GaAs Power MESFET during operation is critical to determining the expected lifetime and overall device reliability.

The polarized liquid crystal technique, which is destructive, has been utilized for estimating device temperatures with a spatial resolution of about $1\mu\text{m}$. On the other hand, non-destructive passive infrared temperature measurement

techniques provide temperature measurements with a spatial resolution of $15\mu\text{m}$, which is too coarse for determining local distribution of state-of-the-art microelectronic device temperatures with submicron gate structures.

We have developed an alternative optical technique based on visible/near infrared emission spectroscopy to provide high resolution, non-destructive channel temperature measurements of the hot spot in the gate channel of a GaAs MESFET.

The development of laser action in crystals doped with magnetic ions has brought a great interest to the field of solid state spectroscopy. The knowledge of the energy levels and transitions of a fluorescent system can be expanded by spectroscopic research. Also the

presence of lattice vibrations gives rise to temperature dependent effects in the observed spectra[1]. Interpretation of these effects can yield information concerning the interaction of host lattice phonons with the electrons on the impurity/doped ions.

An isolated impurity/doped ion in an excited electronic state can decay by three processes: (1) radiative decay through an electronic transition, giving rise to the emission of a photon; (2) radiationless decay through a vibrational transition, giving rise to the emission of phonons; and (3) vibronic decay through a coupled vibrational-electronic transition, giving rise to the absorption or emission of a phonon with the emission of a photon. The inverse of the fluorescence decay time of the excited state will be the sum of the decay probabilities of these three processes. Analogous excitation processes occur in the absorption of light by the impurity or doped ions. Electronic transitions provide information on the energy levels of the impurity ion while radiationless and vibronic transitions provide information on the electron-phonon interaction.[1]

Radiative and vibronic transitions can be observed directly in optical spectra whereas radiationless transitions are observed only indirectly through the temperature dependence of spectroscopic data. Figure 1 shows a diagram of vibronic and radiative transitions in both absorption and emission. The radiative transitions give rise to zero-phonon lines in the spectra. Vibronic sidebands will appear on both the low energy and high energy side of these lines. In absorption spectra the low energy vibronics are due to the concurrent absorption of a photon and a phonon whereas in the fluorescence spectra the low energy vibronics are due to the concurrent emission of a photon and a phonon. Similarly, the high energy vibronics in absorption are due to the simultaneous absorption of a photon and emission of a phonon while in the fluorescence spectra they are due to the simultaneous emission of a photon and absorption of a phonon. Thus, the absorption and emission spectra should appear as mirror images on either side of the zero-phonon line. However, since the intensity of these sidebands is proportional to the probability of absorption or emission of phonons, the low energy absorption vibronics and high energy emission vibronics are

generally not observed at low temperatures where few phonons are available for absorption.

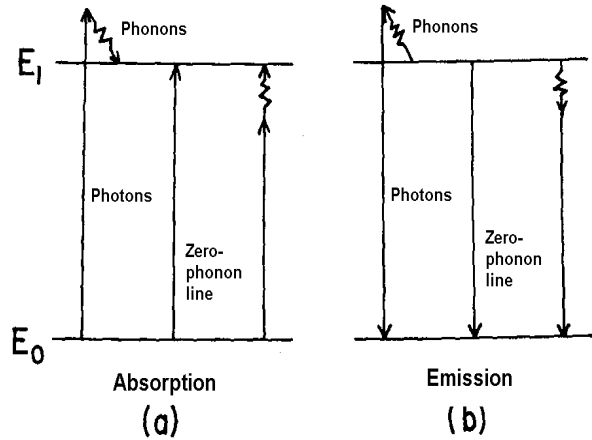


Figure 1. Diagrams of vibronic and radiative transitions for both in absorption (a) and in emission (b) of photons.

Three types of spectral profiles can be observed, depending on strength of the electron-phonon interaction. These are shown in Figure 2 for typical fluorescence spectra. For weak electron-phonon interaction most of the emission occurs purely radiatively. This gives rise to a very intense zero-phonon line with a weak, structured vibronic sideband consisting mostly of one-phonon emission transitions. As the strength of the electron-phonon interaction increases more emission occurs in the vibronic sideband and less in the zero-phonon line. The vibronic bands can be much broader and less structured when multi-phonon transitions are important and in some cases the zero-phonon line is not observed at all. As temperature is increased the relative intensities and shape of the vibronic sidebands change due to the change in the probability of absorbing and emitting phonons. Phonon scattering and radiationless transitions also cause a change in the width and position of the zero-phonon line with temperature.

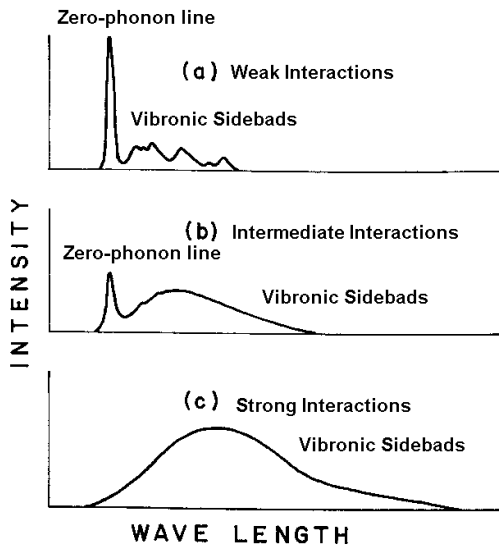


Figure 2. Three types of profiles in optical spectra for weak(a), intermediate (b), and strong (c) electron-phonon/exciton interactions.

There are two purposes for studying the spectra of impurities in solids: to characterize and understand the optical properties of the system; and to obtain information on the phonons of the host crystal and how they interact with the electrons on the impurity. This paper is concerned mainly with the latter purpose. This information on the lattice dynamics is interesting because of the important role played by phonons in the thermal, electrical, and optical properties of solids.

The most powerful technique currently used for studying lattice vibrations is neutron scattering. Despite the wealth of information which has been obtained from this technique, it does have some limitations such as the need for expensive equipment, a relatively low resolution, and the fact some materials cannot be investigated because they have a low scattering cross section or high absorption cross section for neutrons. Infrared absorption and Raman and Brillouin light scattering provide complimentary techniques for investigating lattice vibrations. These methods have higher resolution than neutron scattering but first order phonon processes are limited to the center of Brillouin zone by momentum conservation. Second order processes are not subject to this restriction but it

is usually quite difficult to unfold the combined density of phonon states. These techniques are also limited by rigorous selection rules.

Perhaps the most attractive feature of vibronic spectroscopy for investigating lattice vibrations is that, compared with the other methods, it is a very simple and inexpensive experimental technique[2]. It also has been shown that information on phonon eigenvectors as well as eigenfrequencies can be obtained from vibronic studies, which is not available by other methods [3]. Phonons from all parts of the Brillouin zone may be active in vibronic transitions although they are subject to certain selection rules. These phonons can be identified even though it is sometimes quite complicated to do so. One of the major problems in using vibronic spectra is that the presence of an impurity center may perturb the lattice modes or introduce local vibrational modes which must be distinguished from the normal lattice modes.

It is important to note that the structure observed in vibronic spectra represents an effective phonon distribution (weighted by the electron-phonon interaction) and not the actual phonon density of states of the crystal. This information is useful itself in understanding the absorption and luminescence properties of the systems and how they change with temperature. It is also possible to use this data to obtain information concerning the lattice dynamics of the host crystal. However, this involves determining the frequency dependence of the electron-phonon coupling parameters. Two methods have been used to do this: One is to assume a simple model for the coupling parameters and use the long wavelength limit of their frequency dependence [4]. This can then be divided out of the measured effective phonon distribution leaving the phonon density of states of the pure crystal. The second method is to formulate from first principles a lattice dynamic model for the crystal with an impurity and from this calculate the predicted shape of the vibronic sidebands[3]. This is by far the most elegant technique for interpreting vibronic spectra and using it makes vibronic spectroscopy the most powerful method for studying lattice dynamics. However, this is a very complicated procedure and to avoid the use of many adjustable parameters in the model it is necessary to have a significant amount of other experimental data available on the crystal. In many cases the first, simpler method gives a good approximation to the true phonon density

of states. It should be noted that all of the information on lattice phonons is contained in the one-phonon sideband and in both techniques this must first be projected out of the total observed vibronic spectra.

Based on the theory of lattice dynamics, band shifts and broadening of solid state semiconductor device crystal materials due to temperature variation have been well understood in principal. The thermal shift of a radiative optical spectral line is the statistical algebraic sum of the shifts of the two levels involved in the transition allowed by the selection rules of the electron-phonon interaction as shown in equation (1).

$$\delta E_i = \sum_j \langle i | H' | j \rangle \langle j | H'' | i \rangle / (E_i - E_j) + \langle i | H'' | j \rangle, \quad (1)$$

Where

$\langle i |$ ($\langle j |$) and E_i (E_j) are the initial (intermediate) quantum states and energy levels,

$$H' = iV_1 \sum_q (h\omega_q/4\pi Mv^2)^{1/2} (b_q - b_q^+),$$

$$H'' = -V_2 \sum_{q,q'} (h/4\pi Mv^2)^{1/2} \omega_q \omega_{q'} (b_q - b_q^+) (b_{q'} - b_{q'}^+), \text{ and}$$

$$H = H_{latt} + H_{ion,exc} + H_{int},$$

Where

$$H_{latt} = \sum_k (h\omega_k)^{1/2} (a_k a_k^+ + 1),$$

$$H_{ion,exc} = H_o + H_{cryst} + H_{so},$$

$$H_{int} = V_1 \epsilon + V_2 \epsilon^2 + \dots,$$

$$\epsilon = iV_1 \sum_q (h\omega_q/4\pi Mv^2)^{1/2} (b_q - b_q^+),$$

H : ion-vibration interaction Hamiltonian,
 h : Plank's constant,
 V_1, V_2 : interaction matrix constants,
 ω_k, ω_q : photon and phonon frequency,
 M, v : Mass and velocity of the electron,
 a_k, b_q , and a_k^+, b_q^+ : annihilation and creation operators of photons and phonons.

However, the crystalline field at the ion, varying in time with the thermal lattice vibrations (phonons) of the neighboring ions, sets up an interaction between the ionic system and the normal modes of the lattice vibrations in the

semiconductor lattice. The lattice vibrations include the local vibrational modes and the neutral excited mobile states (excitons) of a crystal bound to neutral donors and acceptors in doped semiconducting materials. Such interaction information obtained from spectral lines has been used in the past to explain the temperature dependence of the relaxation time of crystal ions in semiconductor band structures, as shown in Figure 3. The width of a spectral line is the statistical sum of the energy spread of the two energy levels involved and may also be broadened by the same mechanisms. [5-7]

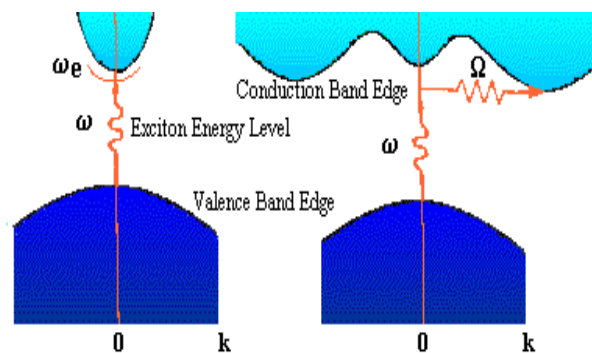


Figure 3. Direct and indirect band structure of semiconductor device materials, involved in optical emission including photons (ω), phonons (Ω) and excitons (ω_e).

Many reports have appeared identifying various photoluminescence (PL) emission characteristics in GaAs multiple-quantum well devices. The spectral characteristics involving the intrinsic and extrinsic radiative recombination of free excitons have been well established to explain the device material quantum-well structures. The intrinsic emissions of the excitons have been observed even at room temperature as dominant radiative transitions. [8-9] The temperature dependence PL spectra of many different GaAs devices can be found elsewhere. [10-11]

One of the many practical applications of this spectral dependence of band shifts and broadening of device materials upon device temperatures is to predict the temperature of a powered device by calibrating an unpowered device at different controlled temperatures. The

true operating temperature of the micron-size powered GaAs MESFET local channel can then be found by measuring the shifts of the spectral band of the multi-quantum well devices.

In this paper we describe a novel, nondestructive experimental procedure for channel temperature measurement and then discuss the results of the actual measurements to summarize our conclusions.

Experimental

The thermal dependence on PL from semiconductor material has been well understood in principle, but it has been difficult to utilize optical techniques to measure the emission spectrum from a fabricated device until the advancement of optical manipulation techniques and computer image processing technology. The technology can now precisely locate a one-micron diameter exciting laser beam, such as a helium-neon laser, on positions of IC components that are most vulnerable to thermal degradation due to high power or stress. The PL light collected nondestructively from a specific component of a fabricated device at cooled (84.8 K) and room temperature can then supply device information, including the temperature profile of the device component. The cooling was achieved by the miniature Joule-Thomson refrigerator from MMR Technologies, Inc.

This method utilizes the latest optical manipulating system, triple grating spectrophotometer technology and up-to-date computer image processing techniques to precisely locate the emission source of the ICs most vulnerable to power system operation. [12-13] A dual micromanipulator is coupled to a thermoelectrically cooled photomultiplier tube (PMT), wavelength scanning system, and conventional lock-in amplifier to detect and amplify the extremely fine device response or photoluminescence (PL) light of the IC gate materials. Computer data processing techniques were employed to boost system sensitivity for signal analysis.

Figure 4 shows a diagram of the PL measurement system. The technique uses a well-focused incident laser beam to generate electron-hole pairs in the semiconductor gate material.

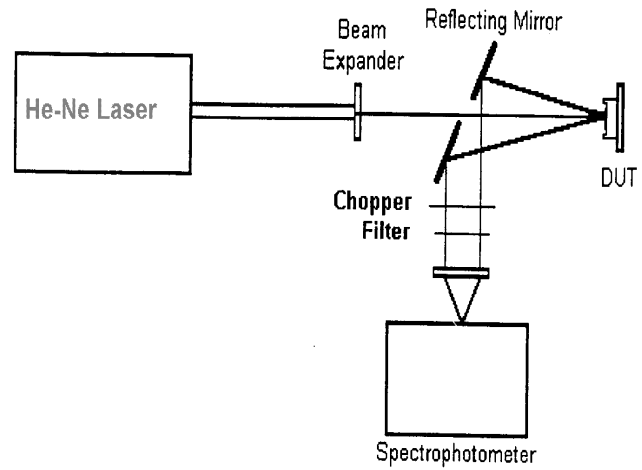


Figure 4. Diagram of channel temperature measurement system.

The basic setup consists of three major parts: (a) an optical probing stage with a microscope, (b) a gated monochromatic-intensifier with a cooled photomultiplier tube and, (c) data processing and control computer. The micromanipulator adjusts a specific gate portion of a device under test onto the miniaturized focused probing helium-neon ion laser beam. This allows the illuminating photons to excite the valance band electrons to conduction bands in the active channel of the GaAs MESFET. Some of the free electrons and holes will bind together to form excitons near the doping ions next to the conduction bands. Some of these impurity bound excitons will be de-excited into the valence band by interacting with the excitons and the lattice phonons. When this transition occurs the photons will be emitted in all directions. The spectrophotometer monitors the emission spectrum modulated by the excitons near to the conduction bands. The emission exciton bands will be modulated by the lattice phonons, which represent the temperature information of the microelectronic device under tests. The spectrophotometer used for these tests was Jarrell-Ash Monspec 27. A thermoelectrically cooled photomultiplier tube (Hamamatsu R943-02/RCA 31032) was used for

the detection of the spectrophotometer. The detected signal was preamplified by an Ithaco Model 164 prior to being fed into an Ithaco Dynatrac 393 Lock-In amplifier. The whole system was controlled by a personal computer. This system was also equipped with an electronic strobing or grating capability, so that it could determine the timing of the device performance and band edges of optical emission.

A micromanipulator stage with a resolution of 0.1 μm was used to position the device under test so that the laser beam exclusively impinges at the desired position of the device. Light emitted from the illuminated spot on the device was reflected by a beam splitter to a chopper and then focused onto the spectrometer slit. The light signal was also low-pass filtered to discriminate against illuminating laser wavelength. The output of the lock-in amplifier is digitized, and then processed in a personal computer to obtain the spectrum of infrared emission stimulated by the laser beam.

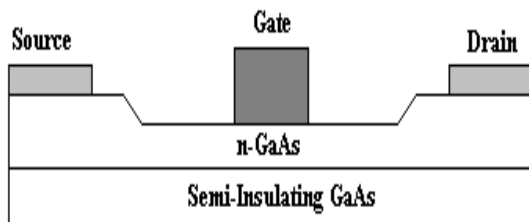


Figure 5. Cross-section of a typical GaAs MESFET.

The GaAs power MESFETs (see Figure 5) used for this investigation were mounted on a Cu/W carrier, and the JPL hybrid laboratory bonded the wires for controlling gates and power supply.

Results and Discussion

The emission spectrum of commercially available GaAs MESFETs was reproduced to identify the reported donor bounded exciton bands with no power applied, at temperatures of 84.8 and 299.1 K. Not shown in Figure 6, the

emission peak at a wavelength of 1.41373 eV for the higher temperature (299.1 K) exceeded the emission peak for the lower temperature (84.8 K) by about 16.30 meV.

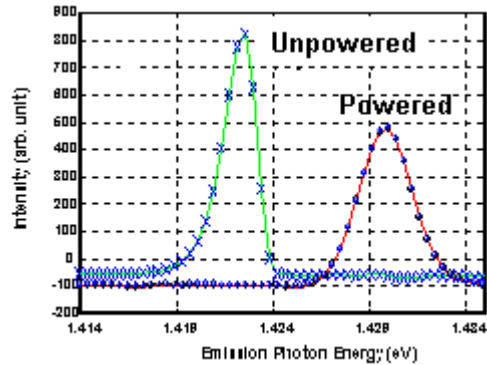


Figure 6. Typical Emission Spectrum of the powered and unpowered GaAs MESFET Gate at 84.8 K.

In another measurement run of the same setup, indicated in the Figure 6, the exterior of the device was maintained at 84.8 K and power was applied; the emission peak of 1.42265 eV for this case was shifted by 7.38 meV from the zero power case at 84.8 K. By linear extrapolation, this wavelength shift indicates that under power, the temperature of the gate rose about 97.3 K above the device operating temperature of 84.8 K.

The obtained results were in general agreement with theoretical calculations [5-8] using equation (2), which is derived from equation (1):

$$E_{cv}(T) - E_{cv}(T_0) = -\alpha(T + \beta) \quad (2)$$

where,

T = Channel Temperature

T₀ = Operating Temperature

E_{cv} = Energy Bandgap

α = Slope of the Extended Plot (Fitting parameter)

β = Debye Temperature (Fitting parameter).

The test system constructed, utilizing for general setup the Microelectronic Advanced Laser Scanner (MEALS), was reported elsewhere [12-13]. Utilizing the micromanipulator stage, a He-Ne laser beam ($\lambda=6238$ Angstrom) with a beam diameter of 0.9 microns was precisely adjusted to the exact gate position (resolution less than

0.1 μm) of the GaAs MESFET device. Discrimination of the emission light signal from the illuminating light was achieved by placing a low-band pass filter between the reflecting mirror (beam splitter) and the spectrometer, as shown in Figure 4. A lock-in amplifier, equipped with a cooled photomultiplier tube, was used for the detection of standard synchronous signals. Data collection and manipulation was performed using a personal computer with the appropriate software tools.

A commercially available GaAs MESFET, with gate dimensions of 0.5 micron (refer Figure 5), was mounted in the test fixture and emission spectra were successfully obtained. The emission spectrum obtained by this test setup, shown in Figure 6, indicates that this technique can be effectively manipulated to collect extremely faint gate emission spectra. The collected emission spectrum (shown in Figure 6) from the free excitons were identified and measured at an operating temperature of 84.8 K. The free exciton emission band shift of the unpowered GaAs MESFET gate was calibrated by the two different temperatures of 299.1 and 84.8 K. The shift was 16.30 meV. In order to remotely measure the local temperature rise of the gate due to the device operation, the emission band shift of the same gate from unpowered to powered were monitored at one (84.8 K) of the calibrated low temperatures. The shift was 7.38 meV.

The technique exploits the temperature dependence of the wavelength of the peak of the stimulated infrared emission spectrum. This wavelength increases approximately linearly with temperature – a consequence of the fact that the energy band gap of these semiconductor material decreases with temperature. Thus, if the temperature dependence of this wavelength is known, it can be used to determine the local temperature in the device while operating at various power levels.

It is well known that the emission bandshift of a semiconductor material is inversely proportional to the material temperature [6-11] due to the first approximation of the electron-exciton interaction at this temperature range. Thus utilizing the bandshifts, one can calculate the localized hot gate temperature rise of the powered device under test. Equation (1) and information summarized in Table I reveal that the localized

hot gate temperature of the device rose by 97.0 K during the operation at 84.8 K. The temperature rise was also compared with the conventional IR measurement technique, which has a resolution between 15 and 100 microns. The average temperature rise with this conventional technique was about 88.8 K. The main difference probably is due to the size of the measurement objective. The temperature rise measured by the infrared radiation technique is not the true local gate temperature but averages temperature of the gate with other parts of the device.

Table I. Summary of band shift data

Test Temperature	Band Position (eV)	Power Applied
299.1K	1.41373	No
84.8 K	1.42265	Yes
84.8 K	1.43003	No

Gate Temperature Rise

$$= T - T_0$$

$$= (299.1 \text{ K} - 84.8 \text{ K}) \times (1.43003$$

$$- 1.42265) / (1.43003 - 1.41373)$$

$$= 97.0 \text{ K.}$$

A lifetime prediction of a device such as power MESFETs is based on the activation energy calculated by a distribution of mean time to failure (MTTF) at different device operating temperatures. One of the most (VENERABLE) portions of the power GaAs MESFETs is the gate. Thus measuring the correct device

operating temperature has a vital impact on product reliability.

Industry-wide implementation of this technique for most semiconductor devices, including silicon devices, requires only minor equipment modifications; the addition of a miniature spectrometer and a refrigerator to the existing micromanipulator under the microscope. The cryogenic system may not even be needed for some semiconductor devices if a known strong impurity spectrum near the band gap is used as the probing tool.

Summary

In this paper, a new non-destructive submicron-size spot temperature assessment technique based on visible/near infrared emission spectroscopy was discussed. It was demonstrated on commercially available GaAs MESFETs and found to have general agreement with calculated results. A non-destructive submicron-size spot laser beam provided by a He-Ne laser was used to excite an extremely small local area of the gate channel of a GaAs MESFET under various operating conditions. The data collected shows a much higher localized "hot spot" temperature of the device than observed using typical IR techniques. This is due to the high-resolution capabilities of this technique. Given the state of the experimental test system, we estimate a spatial resolution of about 0.9 microns and a spectral resolution of about 0.1 Angstroms. This provides 15 - 100 times finer spatial resolution than can be obtained using the best passive IR systems available. The temperature resolution (< 0.02 K/ μm) of this technique depends upon the spectrometer used, and can be further improved.

Acknowledgements

The authors are grateful to their numerous colleagues for providing technical information for this paper including Charles T. Crusan, R. Ruiz, Duc T. Vu, Russel A. Lawton. and James O. Okuno of JPL

The research described in this paper was carried out by the Center for Space Microelectronics Technology, Jet Propulsion

Laboratory, California Institute of Technology, under a contract with the National Aeronautics and Space Administration. Reference herein to any specific commercial product, process, or service by trade name, trademark, manufacturer, or otherwise, does not constitute or imply endorsement by the United States Government or the Jet Propulsion Laboratory, California Institute of Technology.

References

- [1]. Baldassare Di Bartolo, Optical Interactions in Solids, John Wiley & Sons, Inc., New York, 1968.
- [2]. Analysis of the Vibronic Spectrum of Chromium Doped Strontium Titanate, Q. Kim, Richard C. Powell, and T.M. Wilson, *Phys. Rev. B*, 12, p. 5627, 1975.
- [3]. W. E. Born, *Phys. Rev. Vol 185*, 1969.
- [4]. A. A. Maradudin, *Solid State Physics*, Vol. 18, p. 273, edited by F. Zeits and D. Turnbull, Academic Press, New York, 1966.
- [5]. A. Kiel, Thermal Broadening of the Moessbauer Line and Narrow-Line Electronic Spectra in Solids, *Phys. Rev.* 126, p. 1292, 1962.
- [6]. R. H. Silsbee, Thermal Broadening of the Moesbauer Line and Narrow Line Electronic Spectra in Solids, *Phys. Rev.* 128, p.1726, 1962.
- [7]. C. D. Thurmond, The Standard Thermodynamic Functions for the Formation of Electrons and Holes in Ge, Si, GaAs, and GaP, *J. Electrochem. Soc.* 122, p.1133, 1975.
- [8]. M. I. Nathan and G. Burns, Recombination Radiation in GaAs, *Phys. Rev.* 129, p. 125, 1963.
- [9]. J. C. Sarace, R. H. Kaiser, J. M. Whelan and R. C. C. Leite, Injection Luminecsence in GaAs by Direct Hole-Electron Recombination, *Phys. Rev.* 137, p. A623, 1965.
- [10]. R. C. Miller, D. A. Kleinman, W. A. Nordland, Jr., and A. C. Gossard, Luminescence studies of optically pumped quantum wells in GaAs-Al_xGa_{1-x}As multilayer structures, *Phys. Rev.B*, 22, p. 863, (1980)
- [11]. P. W. Yu, S. Shaudhuri, D. C. Reynolds, K. K. Bajaj, C. W. Litton, W. T. Masselink, R. Fischer, and H. Morkoc, Temperature Dependence of Sharp Line

photoluminescence in GaAs-Al_{0.25}Ga_{0.75}As Multiple Quantum Well Structure, *Solid State Comm.*, 54, p. 159, 1985.

- [12]. Q. Kim, and George Soli, Laser Scanner Tests for Single Event Upsets, *NASA Tech Briefs*, 16, p.56 , 1992.
- [13]. S. K. Mendis, S. E. Kemeny, R. C. Gee, B. Pain, Q. Kim, and E. R. Fossum, CMOS Active Pixel Image Sensors for Highly Integrated Image System, *IEEE J. of Solid-State Circuits*, 32, p.187, 1997.

Figure Captions:

Figure 1. Diagrams of vibronic and radiative transitions for both in absorption (a) and in emission (b) of photons.

Figure 2. Three types of profiles in optical spectra for weak(a), intermediate (b), and strong (c) electron-phonon/exciton interactions.

Figure 3. Direct and indirect band structure of semiconductor device materials, involved in optical emission including photons (ω), phonons (Ω) and excitons (ω_e).

Figure 4. Diagram of channel temperature measurement system.

Figure 5. Cross-section of a typical GaAs MESFET.

Figure 6. Typical Emission Spectrum of the powered and unpowered GaAs MESFET Gate at 84.8 K.

Figure 1.

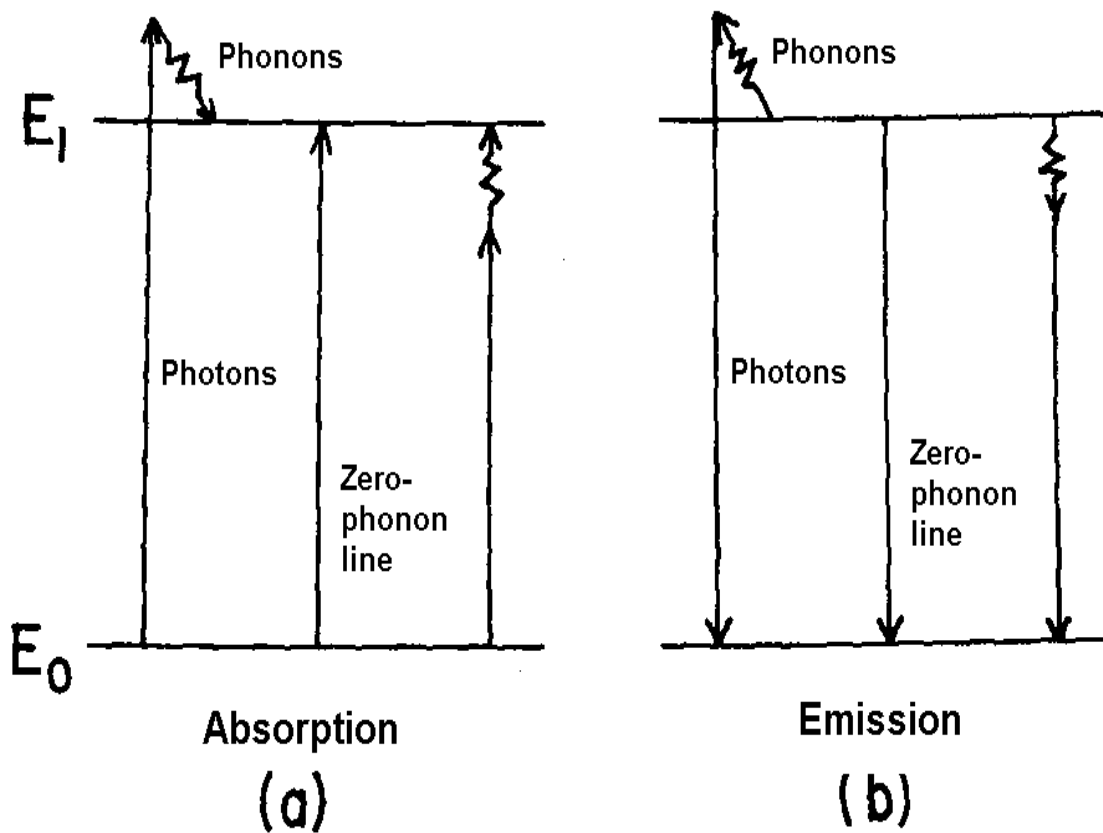


Figure 2.

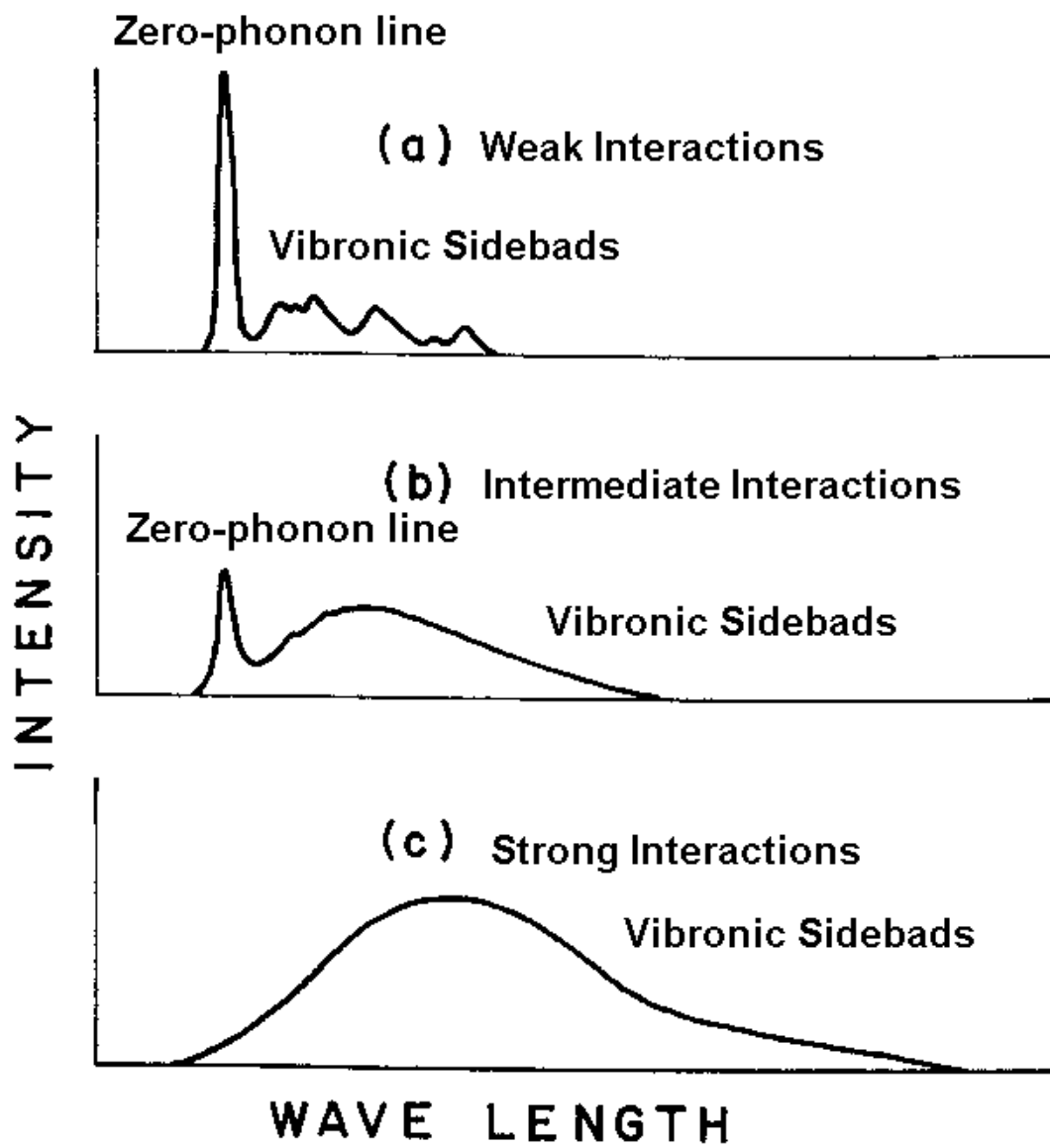


Figure 3.

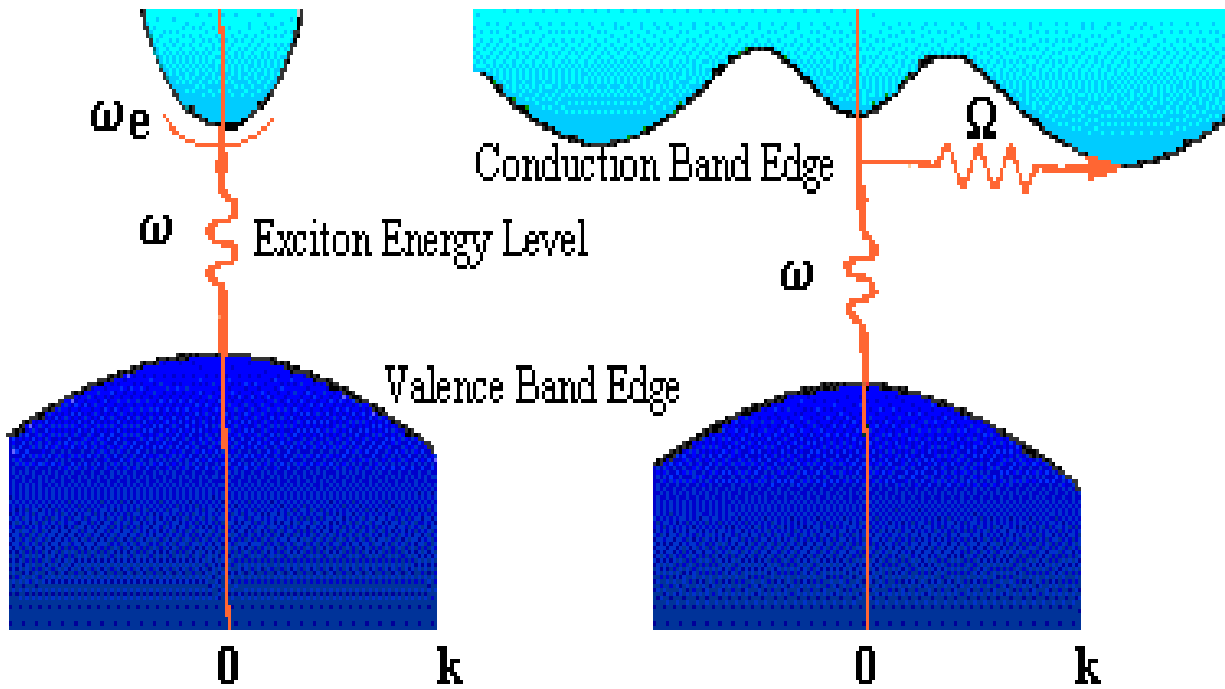


Figure 4.

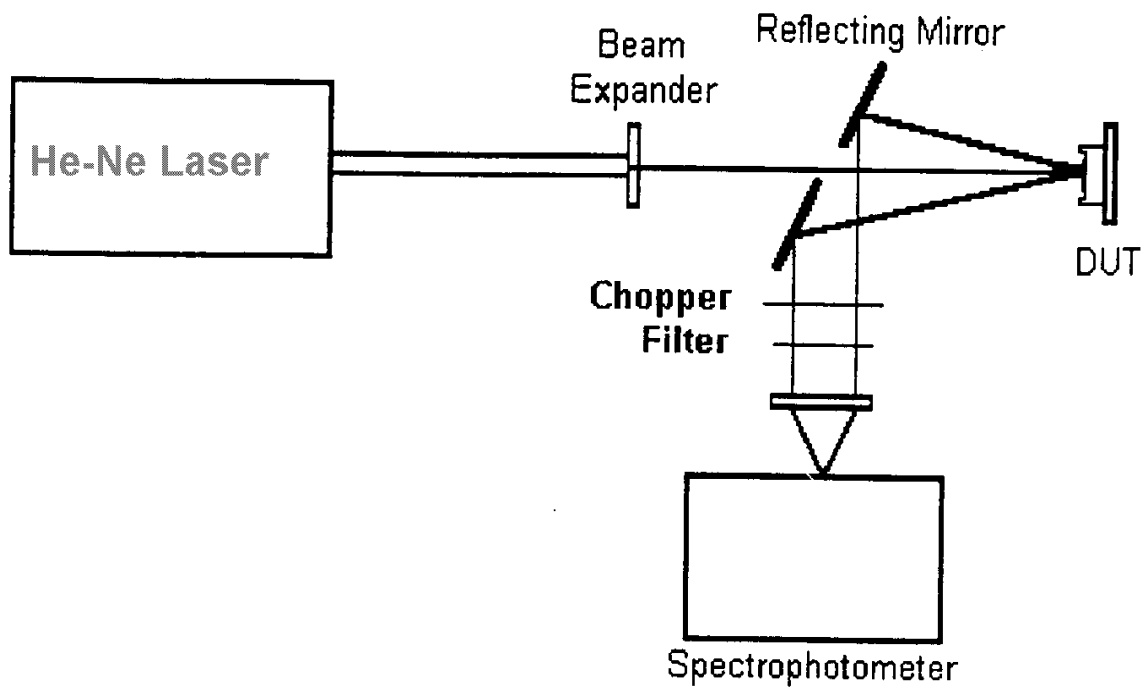


Figure 5.

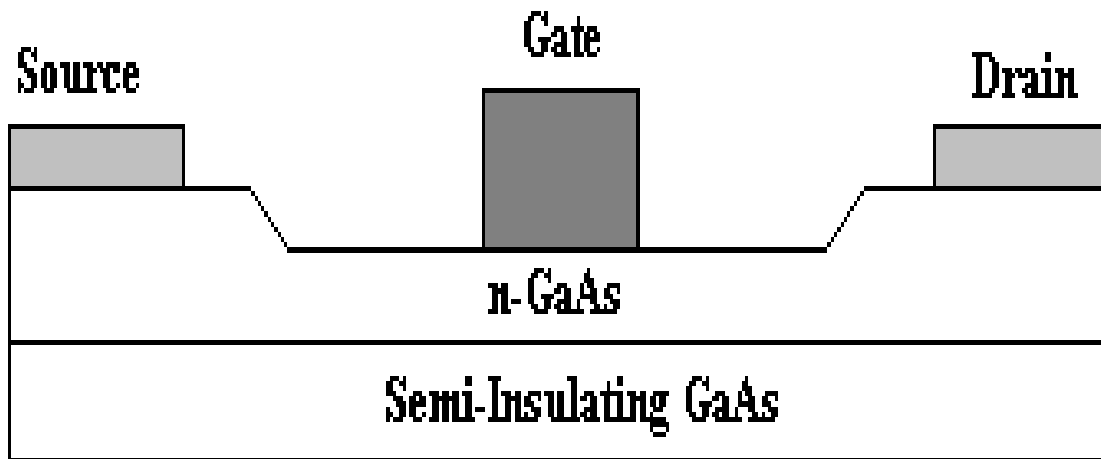


Figure 6.

